

To further understand graph signals

Feng Ji, Wee Peng Tay, *Senior Member, IEEE*

Abstract

Graph signal processing (GSP) is a framework to analyze and process graph-structured data. Many research works focus on developing tools such as Graph Fourier transforms (GFT), filters, and neural network models to handle graph signals. Such approaches have successfully taken care of “signal processing” in many circumstances. In this paper, we want to put emphasis on “graph signals” themselves. Although there are characterizations of graph signals using the notion of bandwidth derived from GFT, we want to argue here that graph signals may contain hidden geometric information of the network, independent of (graph) Fourier theories. We shall provide a framework to understand such information, and demonstrate how new knowledge on “graph signals” can help with “signal processing”.

Index Terms

Graph signal processing, signal types, smooth graph signals

I. INTRODUCTION

Since its emergence, the theory and applications of graph signal processing (GSP) have rapidly developed [1]–[13]. Many different aspects of GSP have been explored. GSP is based on the choice of a graph shift operator (GSO), and the cornerstone of GSP is *graph Fourier transform* defined using the GSO [1], [2]. This allows us to introduce *frequency domain*, analogous to the classical Fourier theory. A well-studied topic in GSP is the *theory of filtering* [2], [11]. Graph filters are fundamental tools to analyze and process graph signals. Many important topics stem from the theory of filtering, including *sampling theory* [14]–[18] and *graph neural networks* [7], [8]. The article [11] contains a comprehensive overview that also discusses many other related topics such as signal reconstruction, graph learning, and applications of GSP.

The authors are with the School of Electrical and Electronic Engineering, Nanyang Technological University, 639798, Singapore (e-mail: jifeng@ntu.edu.sg, wptay@ntu.edu.sg.)

Suppose a graph G is of size n . According to the definition, a graph signal f is a vector in \mathbb{R}^n , with each component corresponding to a node of the graph. There is no reasonable interpretation of f without the graph G . The above-mentioned works take care of the “signal processing” aspect of GSP, by leveraging the fundamental assumption that the signal value should be close to each other at any pair of nodes connected by an edge. From here, we see that the property of the signal f with respect to (w.r.t.) the graph G plays a central role. Motivated by such a consideration, in this paper, we focus solely on the “graph signal” aspect of GSP. To be more precise, we want to describe how we may quantify the notion of “smoothness” of graph signals. Based on such a notion, we can give a characterization of graph signals. To do so, we want to dig out hidden geometric information contained in graph signals and compare such information with the geometry of the given graph.

Classically, many research works rely on the notion of bandlimitedness [18]–[22] to characterize graph signals, with tasks ranging from sampling, and signal reconstruction to topology learning. A signal with small bandwidths is considered to be smooth. However, it is arguable whether such consideration is most appropriate or not. For example, in the first place, bandlimitedness does not only depend on the graph but also relies heavily on the choice of the GSO, for which we have quite a few candidates. Moreover, for most of the common choices of GSO, smooth signals are those whose values are close to each other at any pair of nodes connected by an edge, as we described earlier. However, signal values between nodes further away are not directly compared. The approach taken in our paper shall address such shortcomings.

To set a few humble goals, we want to:

- Develop new methods to identify hidden geometric information of graph signals.
- Use these methods to explicitly define the smoothness of graph signals.
- Classify graph signals based on the new notion of smoothness.
- Investigate new insights into GSP by combining a new understanding of graph signals with classical GSP tools.

Each of these goals is fully explored in a section of the paper, and the rest of the paper is organized as follows. We motivate our goals and approach in Section II. We realize that besides from being either smooth or noisy, a graph signal can have other characterizations that agree with neither. For example, as we demonstrate with an example, a signal can look noisy but contains important geometric information. We coin the term “perpendicular signal” for such a signal. To understand perpendicular signals, we propose to take an indirect route and study a quantitative

notion of smoothness. In Section III, we describe the framework to compare a graph and signals by using an explicit geometric construction. The framework us allows to formally define the smoothness of graph signals in Section IV. We present simulation results in Section V. The focus is to combine our investigation of signals themselves with well-established GSP tools, to shed light on new insights into GSP theory. We finally conclude in Section VI. All proofs are contained in the Appendix.

II. GRAPH SIGNAL TYPES

Let $G = (V, E)$ be a finite unweighted simple graph of size $n = |V|$, where V is the vertex set and E is the set of edges of G . A *graph signal* f is a function $f : V \rightarrow \mathbb{R}$. An equivalent interpretation is to view f as an n -dimensional vector, where the component corresponding to $v \in V$ is denoted by $f(v)$. There have been numerous studies of graph signals with the theory of graph signal processing (GSP). One of the central themes is the study of *bandlimited graph signals*. Intuitively, the notion is a discrete analog of its counterpart in classical Fourier theory. Such a signal is considered to be smooth in the sense that the signal values at neighboring nodes are close to each other. On the opposite side, we have *noises*, whose signal values fluctuate widely even across neighboring nodes. There are statistical models for noises []. In general, they are regarded as obstacles in graph signal processing. In the next example, we want to discuss the possibility of scooping up useful information from “noises”. The key observation is that a seemingly noisy graph signal may contain geometric information that supplements the graph structure.

Example 1. Consider a helix curve (a spiral in \mathbb{R}^3 as in Fig. 1) C given by the parametric form

$$C(t) = (x(t), y(t), z(t)) = (\cos t, \sin t, t), t \in [0, 5\pi].$$

Assume that n is chosen such that $5 \nmid n-1$. We take n uniformly spaced points $V = \{v_1, \dots, v_n\} \subset C$ with $v_1 = C(0)$ and $v_n = C(5\pi)$. The set V together with their connections on C gives rise to the path graph P with n nodes. On the other hand, we may equivalently encode all information in a different graph G and a signal f as follows.

We apply the projection p of V to the (x, y) -plane. Based on their proximity on the unit circle, we have a cycle graph G on n -nodes $u_i = p(v_i), 1 \leq i \leq n$. The condition $5 \nmid n-1$ ensures $u_i \neq u_j$ for $i \neq j$. We construct a graph signal f on G such that $f(u_i)$ is the height of v_i , i.e., $f(u_i) = 5(i-1)\pi/(n-1)$. As C spirals multiple rounds, there are nodes close to each other

on G whose f values differ much. Hence, f resembles a noise. However, if we disregard the geometric information contained in f , we may have a wrong interpretation of both G and f . In such cases, applying GSP tools to f viewed as a signal on G becomes inappropriate. However, G and f combined do contain full information about the original setup. Moreover, we observe that f is placed in the direction perpendicular to G .

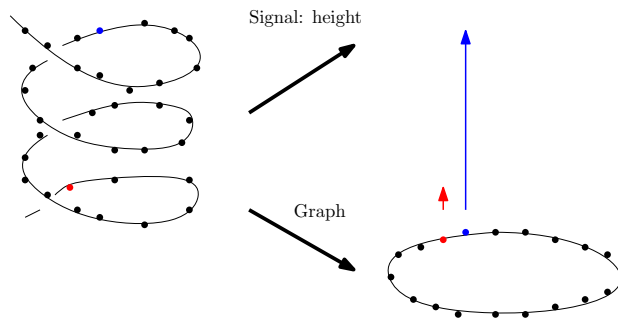


Fig. 1. The helix curve.

To give more intuitions, we discuss two different ways to interpret graph signals. Classically, one chooses a graph shift operator (GSO) A and constructs a filter bank from it, such as the convolution filters, and band-pass filters. Given a graph $G = (V, E)$ and a signal f , one applies filters from a filter bank to f , for analysis purposes. This is the *function point of view* of graph signals, namely we study properties of f using the geometry of G encoded in A .

On the other hand, we may also consider the *geometric point of view* of graph signals. Namely, we view f as mapping the nodes V into \mathbb{R} . This should provide additional geometric information of V other than that contained in E . In particular, if such additional information is not coherent w.r.t. that of E (e.g., Example 1), applying filters constructed from G to analyze f becomes inappropriate.

The function point of view focuses on understanding graph signals. We should expect that the function point of view gives a more accurate understanding provided that the structure of G is more accurate. On the other hand, the geometric point of view provides us with a means to enhance our knowledge of the graph structure. In summary, we want to explore geometric information contained in graph signals as a central theme.

By Example 1, we see describing non-smooth graph signals as noise can cause information loss. The seemingly noisy signal in the example is in the perpendicular direction to the planar

embedding of the graph. This prompts us to introduce the notion of perpendicular graph signals.

Definition 1. *Let S be a subset of graph signals. Then the space of perpendicular graph signals w.r.t. S is the orthogonal complement S^\perp of S .*

Though we have a seemingly naive notion here, the real point is that the set S contains those signals coherent with the graph structure, such that it makes sense to analyze them with current GSP techniques. Such a signal is considered as “smooth”, which will be made explicit in Section IV. On the other hand, a signal f in S^\perp contains geometric information “perpendicular” to that offered by G (c.f. Example 1). Hence, we may consider using f to enhance our understanding of G , instead of processing it with filters built from G . According to Definition 1, smooth signals and perpendicular signals are the two sides of the same coin. Our strategy is to focus on the former explicitly in Section IV.

We end this section by providing further intuitions and heuristics. We describe some major challenges to “compare the geometry of graph and signal”, which motivate subsequent sections.

To proceed, we introduce a notion here. Suppose $f = (f_i)_{1 \leq i \leq n}, g = (g_i)_{1 \leq i \leq n} \in \mathbb{R}^n$. For convenience, the notation is only used till the end of this subsection. We say that f *interlaces* g if there is a constant c such that $h = f + c$ satisfies $g_i \leq h_i \leq g_{i+1}$ for $1 \leq i \leq n - 1$, $h_n \geq g_n$ and $h_1 g_1 + h_n g_n \geq 0$. Notice that the last condition loosely controls the absolute values of g_1 and h_n .

Lemma 1. *For $n \geq 3$, suppose $f, g \in \mathbb{R}^n$ are nonzero vectors and g is orthogonal to constant vectors. If a re-arrangement of indices makes f interlace g , then f and g are not orthogonal to each other.*

Let us try to interpret “ f interlaces g ” geometrically. According to the definition, the increments in the signal values $f_{i+1} - f_i$ are controlled by those of g . In particular, if the increments are small for g , so are those for f . On the other hand, if f does not interlace g , then we can observe large increments for f can occur when we have a small increment in g . In the GSP setting, one argues heuristically that a smooth signal is the one that has a small increment across many direct edges. Therefore, if we have a set S exhausts smooth signals, then any f perpendicular to S does not interlace any of the signals in S . Based on our discussions, such f tends to violate having small increments along a direct edge for many different edges.

However, to make our discussion rigorous, we need to specify what we mean by a signal being

smooth, aside from the hand-waving description as above. The main challenge is that signals and graphs are different mathematical objects. Therefore, they are not directly comparable. Our key task is to set-up a common platform so that we can discuss the geometric contents of both graphs and signals and make comparisons.

III. GRAPH-SIGNAL COUPLING

As we have pointed out in the previous section, a graph signal can contain geometric information not captured by the graph. In this section, we shall discuss a framework, called *graph-signal coupling*, to extract geometric information from graphs and signals combined.

A. An axiomatic approach

We want to first propose an axiomatic approach to avoid restricting to a single construction, while we still give an explicit construction in the next subsection. The axiomatic approach proceeds by stating a few desired properties any construction needs to satisfy. We start by motivating such properties.

Recall that we want to find a “common platform” to compare graphs and signals. More specifically, let \mathcal{S} be a set of objects having geometric interpretation. For example, \mathcal{S} can be the set of graphs or the set of finite (pseudo) metric spaces (recall in a pseudo metric space, $d(x, y) = 0$ does not imply $x = y$). Suppose $F = \{f_1, \dots, f_m\}$ contains a finite set of signals on G . We want to produce an object $G_F \in \mathcal{S}$.

First of all, we *need a notion of equivalence* between objects in \mathcal{S} , and the reason is as follows. Suppose G_1 and G_2 are isomorphic graphs by a permutation σ of the nodes. For F_1 on G_1 , permuting (with σ) the indices of each signal in F_1 results a set of signals $F_2 = \sigma(F_1)$. The objects G_{1F_1} may not be the same as G_{2F_2} , but they should be equivalent.

The coupling should be extendable to pairs $G_{F_1} \in \mathcal{S}$ and F_2 , where both F_1 and F_2 are finite sets of signals on G . More precisely, we want to have an object $(G_{F_1})_{F_2} \in \mathcal{S}$. This is because regarded as observations, the signals F_1 and F_2 may not be obtained simultaneously. Moreover, we also want that $G_F \in \mathcal{S}$ allows us to recover both the graph and signals to a certain extent.

Keeping these requirements in mind, we now formalize the idea of graph-signal coupling.

Definition 2. *Let \mathcal{G} be the set of graphs. A graph-signal coupling consists of the following data: a set of objects \mathcal{S} and an equivalence relation “ \sim ” on \mathcal{S} . For each graph G and a finite set of*

signals F , there is a $G_F \in \mathcal{S}$ (if $F = \{f\}$, we write G_f for G_F for convenience) such that the following holds:

- 1) *Composability*: For each finite set of signals F' , there is $(G_F)_{F'} \in \mathcal{S}$.
- 2) *Commutativity and associativity*: $(G_F)_{F'} \sim G_{F \cup F'}$.
- 3) *Recoverability of G* : There is base map $b : \mathcal{S} \rightarrow \mathcal{G}$ such that $b(G_F) = G$.
- 4) *Recoverability of signal*: $G_f = G_{f'}$ implies $|f(v_i) - f(v_j)| = |f'(v_i) - f'(v_j)|$, $1 \leq i, j \leq n$.
Moreover, if $f = af' + c$ for scalar $a \neq 0$ and constant signal c , then $G_f \sim G_{f'}$.

Before presenting an explicit construction in Section III-B, we analyze the obvious choice of \mathcal{S} being the collection of graphs. This means for a graph G and a finite set of signals F , we need to produce a new graph G_F . In the collection of graphs, the most reasonable notion of equivalence is graph isomorphism. Two isomorphic graphs are essentially the same up to a re-ordering of vertices. In addition, for any G and a constant signal c , it is reasonable to require G_c isomorphic to G . Consider any signal f . Condition 2) forces $(G_f)_f$ isomorphic to G_f . The latter in turn is isomorphic to $(G_f)_c$ for any constant signal. This means that on the graph G_f , we are not able to differentiate f from any constant signal, i.e, the recoverability of signals is violated.

If we examine the above argument, we notice that the cause of the problem is that equivalence on our current choice of \mathcal{S} is too restrictive. As a remedy, we shall consider that \mathcal{S} contains a parametrized family of graphs in Section III-B.

B. An explicit construction

In this subsection, we give an explicit construction that verifies the properties listed in Definition 2. The construction is inspired by the basic construction in linear algebra: taking the sum of perpendicular vectors.

In the construction, an object in \mathcal{S} is a parametrized family of graphs. More precisely, it is a map $\gamma : M \rightarrow \mathcal{G}$, where M is a parameter space such as a topological space or a manifold, and \mathcal{G} is the collection of finite graphs. For convenience, we use γ to denote such an object.

Given $\gamma_i : M_i \rightarrow \mathcal{G}$, $i = 1, 2$, a *morphism* from γ_1 to γ_2 is a map $\phi : M_1 \rightarrow M_2$ such that $\gamma_1 = \gamma_2 \circ \phi$ (illustrated in Fig. 2). If M_i are topological spaces, we usually require ϕ to be continuous; and if M_i are differentiable manifolds, we want ϕ to be differentiable. To understand this notion, consider $g \in \text{Im}(\gamma_1)$, i.e., $g = \gamma_1(x)$ for $x \in M_1$. Then $y = \phi(x)$ satisfies $\gamma_2(y) = g$.

Intuitively, this indicates that ϕ is analogous to a “surjection” from γ_2 to γ_1 , though we notice a reverse of domain and codomain. Now we proceed to define the equivalence relation.

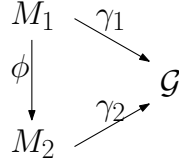


Fig. 2. Schematic diagram of a morphism.

Definition 3. Given γ_1, γ_2 , we write $\gamma_1 \leq \gamma_2$ if there is a morphism ϕ from γ_1 to γ_2 . We say γ_1 and γ_2 are equivalent to each other, denoted by $\gamma_1 \sim \gamma_2$ if $\gamma_1 \leq \gamma_2$ and $\gamma_2 \leq \gamma_1$.

The equivalence is based on the analogy that two finite sets are equivalent to each other if either surjects onto the other.

We can now define G_F for given graph G and a finite set of signals $F = \{f_1, \dots, f_k\}$. Let $M_F = \mathbb{R}_{\geq 0}^{k+1}$. We write $x = (x_0, x_1, \dots, x_k)$ for a typical element in M_F .

Then $G_F \in \mathcal{S}$ is a map $G_F : M_F \rightarrow \mathcal{G}$ defined by¹

- 1) For two nodes u, v , compute

$$\Delta(u, v) = \left(\sum_{1 \leq i \leq k} x_i (f_i(u) - f_i(v))^2 + d_G(u, v)^2 \right)^{1/2},$$

where d_G is the distance on G .

- 2) In $G_F(x)$, a pair of nodes u, v is connected by an edge if $\Delta(u, v) \leq x_0$.

Intuitively, $x_i, 1 \leq i \leq k$ scales the difference measured by the signal f_i . The parameter x_0 is a threshold to determine the connections in $G_F(x)$. Of course, we need to check the following.

Theorem 1. Associating G, F with $G_F : M_F \rightarrow \mathcal{G}$ is a graph-signal coupling.

C. The abstract picture

In this section, we give a more abstract description of the picture, to explain the theoretical underpinning of our approach.

¹The construction is inspired by the idea of [23] Definition 2.5.

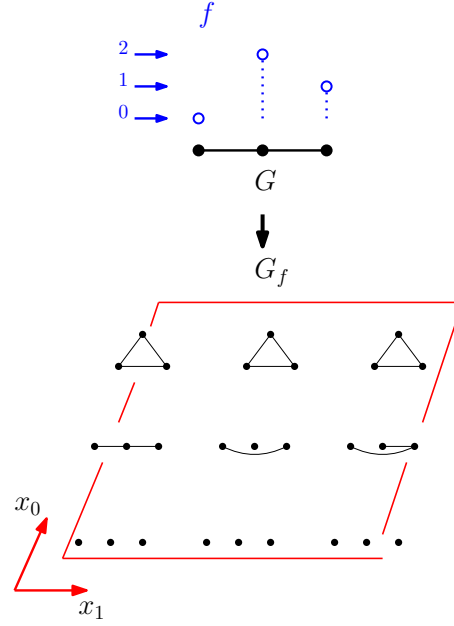


Fig. 3. In this example, G is the path graph on 3 nodes, and the signal f is $(0, 2, 1)^T$. As shown below, G_f is the parameter family of graphs. There are two parameters (x_0, x_1) . The parameter x_1 scales signal differences and x_0 serves as a threshold to determine edge connections.

Let \mathcal{G}_n be the collection of unweighted, undirected finite graphs on n vertices. We start with an object G in this collection. On the other hand, we want to study signals on such a graph G . The collection of such signals can be identified with \mathbb{R}^n , denoted by \mathcal{F}_n . As we propose in this paper, we want to investigate geometric information contained in a signal $f \in \mathbb{R}^n$. While a direct comparison of f and G is obscure as they belong to different collections of objects, we want a common, new collection of objects that enlarges both \mathcal{G}_n and \mathcal{F}_n .

Proposition 1. Introduce

- \mathcal{M}_n : the collection of metric spaces of size n ;
- \mathcal{MG}_n : the collection of map $\phi : M \rightarrow \mathcal{G}_n$, i.e., as a parametrized family of graphs, by a topological space M such that $Im(\phi)$ is finite; and
- \mathcal{SG}_n : the collection of a finite sequence of undirected, unweighted graphs of size n .

Then we have the diagram of maps as shown in Fig. 4 such that $\tau_4 \circ \tau_3 \circ \tau_2 \circ \tau_1 = Id_{\mathcal{G}_n}$, $\tau_2 \circ \tau_1(G) = G_c$ for any constant signal c . Moreover, if $\tau_5(f) = \tau_5(g)$, then $f = g + c$ or $f = -g + c$ for some constant signal c .

As a consequence, we have placed both graphs and signals in the common collections \mathcal{MG}_n

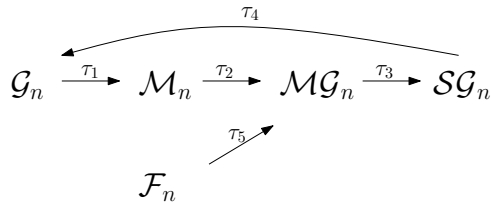


Fig. 4. The schematic illustration of Proposition 1.

and $\mathcal{S}\mathcal{G}_n$, where we can compare them directly.

IV. SMOOTH GRAPH SIGNAL

We have introduced perpendicular signals earlier, which contain additional geometric information. It is supposed to come together with the notion of smooth signals, which we formally define in this section. The main idea is that we make use of the constructions of Section III to place both graph and a signal in a common collection of objects and make comparisons based on an appropriate measure defined on the collection. The first goal is to introduce such a measure.

Let $*$ be the trivial graph on a single node. We also view it as a degenerate graph on n nodes by identifying all of them with the single node, i.e., the distance between any pair of nodes is 0. On the other hand, on the graph G , let c be the unit constant signal.

Recall that according to Section III, we have defined $*_f$ and G_c as objects in some collection \mathcal{S} . By Proposition 1, \mathcal{S} can be either the collection of a parameterized family of graphs or the collection of a finite sequence of graphs.

Definition 4. Assume that there is $d_{\mathcal{S}} : \mathcal{S} \times \mathcal{S} \rightarrow \mathbb{R}_{\geq 0}$. Then for $\epsilon \geq 0$, a graph signal f on G is called ϵ -smooth (w.r.t, $d_{\mathcal{S}}$) if $d_{\mathcal{S}}(*_f, G_c) \leq \epsilon$.

As we pointed out earlier, we want $d_{\mathcal{S}}$ to play the role of a metric to measure how different two elements of \mathcal{S} are. However, the $d_{\mathcal{S}}$ we are going to define does not satisfy all the properties of a metric such as being symmetric.

We now describe an explicit construction of $d_{\mathcal{S}}$ based on our choice of \mathcal{S} and construction of G_F . We only consider elements of \mathcal{S} taking the form of G_F (cf. Section III). Recall that for two unweighted graphs G_1 and G_2 on the same amount of n vertices, their *Hamming distance*

$d_H(G_1, G_2)$ counts the number of edges contained exclusively in either G_1 or G_2 . More generally, if Γ is a set of unweighted graphs on n vertices, then

$$d_H(G_1, \Gamma) = \min_{G_2 \in \Gamma} d_H(G_1, G_2).$$

For G of size n and a finite set of graph signals F , we have constructed $G_F : M_F \rightarrow \mathcal{G}$ such that M_F is a subset of a Euclidean space. The image $Im(G_F)$ is finite. An extreme case in $Im(G_F)$ is the complete graph K_n , and write $Im(G_F)^\circ$ for $Im(G_F) \setminus \{K_n\}$. Let the inverse image of $Im(G_F)^\circ$ has *Lebesgue measure* $|G_F^{-1}(Im(G_F)^\circ)|$.

Suppose G_1 and G_2 are graphs on the same set of ordered vertices V and finite sets of graph signals F_1 and F_2 . For convenience, denote $\gamma_1 = G_{1F_1}$ and $\gamma_2 = G_{2F_2}$. If $Im(\gamma_1)^\circ$ is non-empty define

$$d_S(\gamma_1, \gamma_2) = \sum_{G \in Im(\gamma_1)^\circ} \frac{|\gamma_1^{-1}(G)|}{|\gamma_1^{-1}(Im(\gamma_1)^\circ)|} d_H(G, Im(\gamma_2)), \quad (1)$$

where $|\cdot|$ denotes the Lebesgue measure of the set. If $Im(\gamma_1)^\circ = \emptyset$, then $d_S(\gamma_1, \gamma_2) = 0$. An illustration is shown in Fig. 5.

We now study some basic properties of ϵ -smooth signals.

- Lemma 2.** 1) If f is ϵ -smooth, then so are rf and $f + c$ for any $r \in \mathbb{R} \setminus \{0\}$ and c a constant signal.
- 2) If G is connected, then the set of 0-smooth signals contains only constant signals if and only if G is not a path.
- 3) The map $\mathbb{R}^n \rightarrow \mathbb{R}$, $f \mapsto d_S(*_f, G_c)$ is continuous on the subset of non-constant signals.

We now discuss other means to estimate the parameter ϵ without directly using the definition.

Example 2. In this example, we re-visit Fig. 5. In particular, we want to compute $d_S(\gamma_1, \gamma_2)$ for $\gamma_1 = *_\sqrt{6}f_2 = *_f$ and $\gamma_2 = G_c$, without directly using the definition. The idea here is that instead of considering each graph of $Im(*_f)$, we consider edges in these graphs. More specifically, we order pairs of distinct vertices $\{u, v\}$ increasingly according to $\Delta(\{u, v\}) = |f_2(u) - f_2(v)|$. We obtain the sequence: $Q = (Q_1, \dots, Q_6) : \{v_1, v_2\}, \{v_1, v_3\}, \{v_2, v_3\}, \{v_3, v_4\}, \{v_1, v_4\}, \{v_2, v_4\}$ with the corresponding Δ values 0, 1, 1, 2, 3, 3. We partition Q into 3 parts: $I_0 = (Q_1)$, $I_1 = (Q_2, Q_3, Q_4)$ and $I_2 = (Q_5, Q_6)$.

Notice that in Fig. 5, we see that $Im(G_c)$ contains 3 graphs, and we call them $G^{(0)}$, $G^{(1)}$ and $G^{(2)}$ respectively.

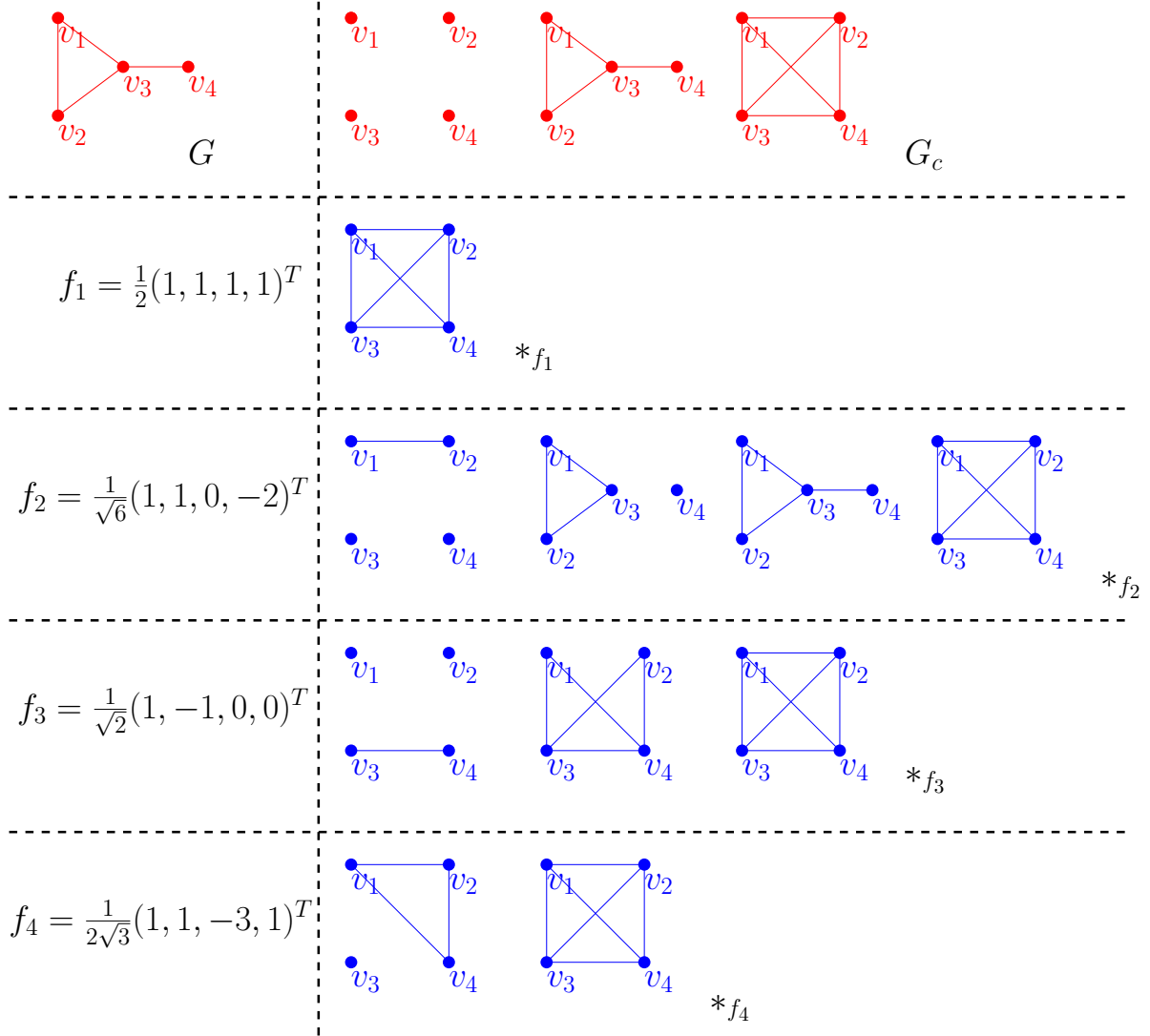


Fig. 5. In this example, G is a graph on 4 nodes. In the top row, we show the image of G_c consisting of a sequence of 3 distinct graphs. On the other hand, we consider an eigenbasis $\{f_1, f_2, f_3, f_4\}$ of the Laplacian of G . In the figure, we show the image of $*f_i, 1 \leq i \leq 4$ in subsequent rows. Using the formula for $d_S(\cdot, \cdot)$, we find that $d_S(*f_i, G_c), 1 \leq i \leq 4$ are $0, 2/3, 1, 3$ respectively.

Now we process each $Q_l, l = 1, \dots, 6$ to obtain a number ϵ_l . We show how this is done for typical examples Q_1 and Q_4 . For $Q_1 = \{v_1, v_2\}$, we notice that the pair first appears as an edge in $G^{(1)}$. We then identify the first pair of I_1 is $Q_2 = \{v_1, v_3\}$. Then we compute $\epsilon_1 = |\Delta(Q_1) - \Delta(Q_2)|/\Delta(Q_6) = 1/3$. Similarly for $Q_4 = \{v_3, v_4\}$, we notice that it first appears as an edge in $G^{(1)}$ as well, and determine Q_2 being the first pair of I_1 . We then find $\epsilon_4 = |\Delta(Q_4) - \Delta(Q_2)|/\Delta(Q_6) = 1/3$. The same computation determines that $\epsilon_2 = \epsilon_3 = \epsilon_5 =$

$\epsilon_6 = 0$. Summing all of them we obtain $\sum_{1 \leq l \leq 6} \epsilon_6 = 2/3$, which is exactly the smoothness of f_2 .

We shall next rigorously describe and then demystify the procedure.

Before formalizing the procedure in Example 2, we make the following technical assumption on f : for two different pairs (as sets) of nodes $\{u_1, v_1\}$ and $\{u_2, v_2\}$, we have $|f(u_1) - f(v_1)| \neq |f(u_2) - f(v_2)|$.

For the graph G , let D_G be its diameter. For each $0 \leq k \leq D_G$, we define $G^{(k)}$ be to the graph on V and u, v is connected by an edge if and only if $d_G(u, v) \leq k$. This sequence of graphs $G^{(k)}, 0 \leq k \leq D_G$ is nothing but the image of G_c .

Suppose we order the distinct pairs of vertices $\{u, v\}$ of V increasingly according to $|f(u) - f(v)|$. In this way, we obtain an ordered sequence of pairs of vertices $Q = (Q_l)_{1 \leq l \leq n(n-1)/2}$, with $Q_l = \{u_l, v_l\}$. A $D_G + 1$ -partition \mathcal{P} of $I = \{1, \dots, n(n-1)/2\}$ is a decomposition of $I = \cup_{0 \leq k \leq D_G} I_k$ into $D_G + 1$ disjoint subsequences of consecutive numbers I_k in I . We assume that the numbers in I_k are smaller than those in I_{k+1} , and we allow I_k to be empty. We compute $\epsilon_{\mathcal{P}}$ as follows.

Algorithm 1

Input: G, f, Q, \mathcal{P} **Output:** $\epsilon_{\mathcal{P}}$ of f

- For each $1 \leq l \leq n(n-1)/2$, let k be the index such that (u_l, v_l) is an edge of $G^{(k)}$ for the first time, in the sequence $G^{(0)}, \dots, G^{(D_G)}$.
- Let l' be first element of I_k and $Q_{l'} = \{u_{l'}, v_{l'}\}$.
- Set

$$\epsilon_l = \frac{||f(u_{l'}) - f(v_{l'})| - |f(u_l) - f(v_l)||}{|f(u_{n(n-1)/2}) - f(v_{n(n-1)/2})|}.$$

- Summing over $1 \leq l \leq n(n-1)/2$,

$$\epsilon_{\mathcal{P}} = \sum_{1 \leq l \leq n(n-1)/2} \epsilon_l.$$

The observation made in Example 2 is demystified by the following result.

Proposition 2. *Let ϵ be the smallest number such that f is ϵ -smooth. Then $\epsilon = \min_{\mathcal{P}} \epsilon_{\mathcal{P}}$, where the minimum is taken over all partitions \mathcal{P} of $I = \{1, \dots, n(n-1)/2\}$ into $D_G + 1$ subsequences.*

Based on the proof of Proposition 2, we can describe the role played by the partition $\mathcal{P} = \{I_0, \dots, I_{D_G}\}$. To compute $\epsilon_{\mathcal{P}}$, we form the sequence of graphs $G_{(l)}$ by including Q_1, \dots, Q_l as edges. In the expression $d_H(\cdot, \cdot)$, we put $G_{(l)}$ with $G^{(k)}$ as the arguments for $l \in I_k$. By the proposition, any choice of \mathcal{P} allows us to obtain an upper bound of ϵ . Moreover, to find the optimal partition, we only need to find the starting and ending indices of each $I_k, 0 \leq k \leq D_G$. This leads to Algorithm 2 that is based on the binary search of such indices.

Algorithm 2

Input: G, f **Output:** \mathcal{P} of f

- Construct $G^{(k)}$ for $0 \leq k \leq D_G$.
 - Form the sequence of pairs of nodes $Q = (Q_l)_{1 \leq l \leq n(n-1)/2}$ with $Q_l = \{u_l, v_l\}$ such that $|f(u_l) - f(v_l)| < |f(u_{l+1}) - f(v_{l+1})|$.
 - For any Q_l , recall $G_{(l)}$ is the graph with edges Q_1, \dots, Q_l .
 - For each $0 \leq k \leq D_G$, apply binary search to Q to find the starting and ending indices of I_k , with the following rule: Then $l \in I_k$ if k is the largest element in $\arg \min_{0 \leq j \leq D_G} d_H(G_{(l)}, G^{(j)})$. Any index l such that Q_l is considered in each iteration is used as a reference index in subsequent iterations.
-

To end this section, we slightly generalize Definition 4. What is missing from the current notion of ϵ -smoothness is that it is not preserved under vector addition. Hence, in general, they do not form a vector space. This is unfavorable in signal processing. On the other hand, Lemma 2 3) shows that if $\epsilon > 0$, in general ϵ -smooth vectors span \mathbb{R}^n . To come up with useful vector spaces, we propose the following.

Definition 5. Suppose $F = \{f_1, \dots, f_n\}$ is an orthonormal basis of \mathbb{R}^n . Then let $F_\epsilon = \{f \in F \mid f : \epsilon\text{-smooth}\}$. An arbitrary signal is ϵ -smooth w.r.t. F if f is in the span of F_ϵ .

If L is a matrix admitting an eigenbasis, then f is ϵ -smooth w.r.t. L if it is ϵ -smooth w.r.t. an eigenbasis of L .

More generally, f is ϵ -smooth if it is in the span of a set of pairwise orthogonal ϵ -smooth vectors.

V. SIMULATIONS

In this section, we provide simulation results. The main focus is to demonstrate that well-established GSP tools can be modified with our new framework to give new insights and

experimental observations.

A. Band-pass filters: old wine in new bottles

In this subsection, we study band-pass filters. We first recall briefly what they are in GSP. Let L be a fixed GSO such as the Laplacian of G . It admits an orthonormal eigenbasis $\mathcal{E} = \{e_1, \dots, e_n\}$ with the corresponding eigenvalues $0 = \lambda_1 \leq \lambda_2 \leq \dots \leq \lambda_n$. For a subset Y of $[n] = \{1, \dots, n\}$, the *band-pass filter* B_Y on any graph signal f is defined as

$$B_Y(f) = \sum_{i \in Y} \langle e_i, f \rangle e_i,$$

where $\langle \cdot, \cdot \rangle$ is the standard inner-product. The band-pass filter retains only the components, indexed by Y , of the eigen-decomposition of f . A slightly more general version is that we take a pair of numbers $\alpha = (\alpha_0, \alpha_1)$, and construct $B_{Y,\alpha} = \alpha_0 B_Y + \alpha_1 I_n$, with I_n the identity map. For example, $B_Y = B_{Y,\alpha}$ for $\alpha = (1, 0)$. The coefficients α provide additional flexibility if we do not want to completely disregard contributions from e_i for $i \notin Y$.

In many tasks, the index set is chosen as $X_m = \{1, \dots, m\}$ for some $m < n$. The resulting filter is called a low-pass filter. It leverages the intuition that structured signals are smooth in the sense that it contains mainly “low frequency” components. Here, “low” refers to small eigenvalues. In our paper, we provide a different interpretation of smoothness as formally defined in Section IV. This allows us to choose an index set according to the smoothness therein. We describe how this simple procedure is done as follows.

Algorithm 3

Input: \mathcal{E}, G, m **Output:** Y_m of size m

- For each $e_i \in \mathcal{E}$, find $\epsilon_i = d_H(*_{e_i}, G_c)$ for any constant signal c .
 - Determine a permutation σ of $1, \dots, n$ according to increasing order of ϵ_i , i.e., $\epsilon_{\sigma(i)} \leq \epsilon_{\sigma(i+1)}$.
 - $Y_m = \{\sigma(1), \dots, \sigma(m)\}$.
-

The index set Y_m constructed in Algorithm 3 shall be used as a substitute of $X_m = \{1, \dots, m\}$ in classical GSP. In general, the resulting filter B_Y is not a low-pass filter in the classical sense. We shall demonstrate with simulations.

We consider the MNIST dataset.² We use a 2D-lattice $G = (V, E)$ to model the graph for each image, and L is the Laplacian of G . As described above, it has an orthonormal eigenbasis $\mathcal{E} = \{e_1, \dots, e_n\}$. We first compute ϵ_i as in Algorithm 3, to investigate the relation between the notions of smoothness introduced in the paper and implicitly suggested by classical GSP. In Fig. 6, we show the plot of ϵ_i (normalized by the size of G) against i . The indices on the horizontal axis are ordered according to the sizes of the eigenvalues of L . Therefore, from the plot, we see that an index i with small GSP frequency does not necessarily have small ϵ_i . As a consequence, Y_m can be very different from the set $X_m = \{1, \dots, m\}$, which is used to construct a low-pass filter in classical GSP. A low-pass filter in terms of size of ϵ_i is a classic band-pass filter, but not necessarily a classical low-pass filter.

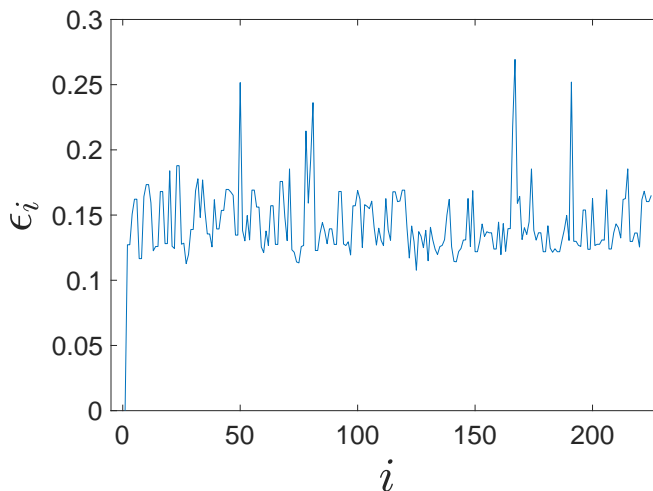


Fig. 6. The plot of ϵ_i against i , where the indices on the horizontal axis are ordered according to the graph frequencies.

We investigate the difference between the band-pass filters with $X_m = \{1, \dots, m\}$ and $Y_m = \{\sigma(1), \dots, \sigma(m)\}$ on processing noisy images, with $m \approx 0.2n$. To do so, we add independent Gaussian noise to each pixel of the samples in the MNIST dataset. We apply appropriate band-pass filters, as denoising functions, to the noisy images to recover the original images. To be flexible, the filters are $B_{X_m, \alpha}$ and $B_{Y_m, \alpha'}$ as described at the beginning of this subsection. Both coefficient sets α and α' , as hyperparameters, are tuned based on a small number of samples. In Fig. 7, we show the results. We see that with $B_{Y_m, \alpha'}$, the recovered images look more like the

²<http://yann.lecun.com/exdb/mnist/>

original ones (especially the complement of the digit figures) as compared with those recovered with $B_{X_m, \alpha}$, which is the classical low-pass filter.

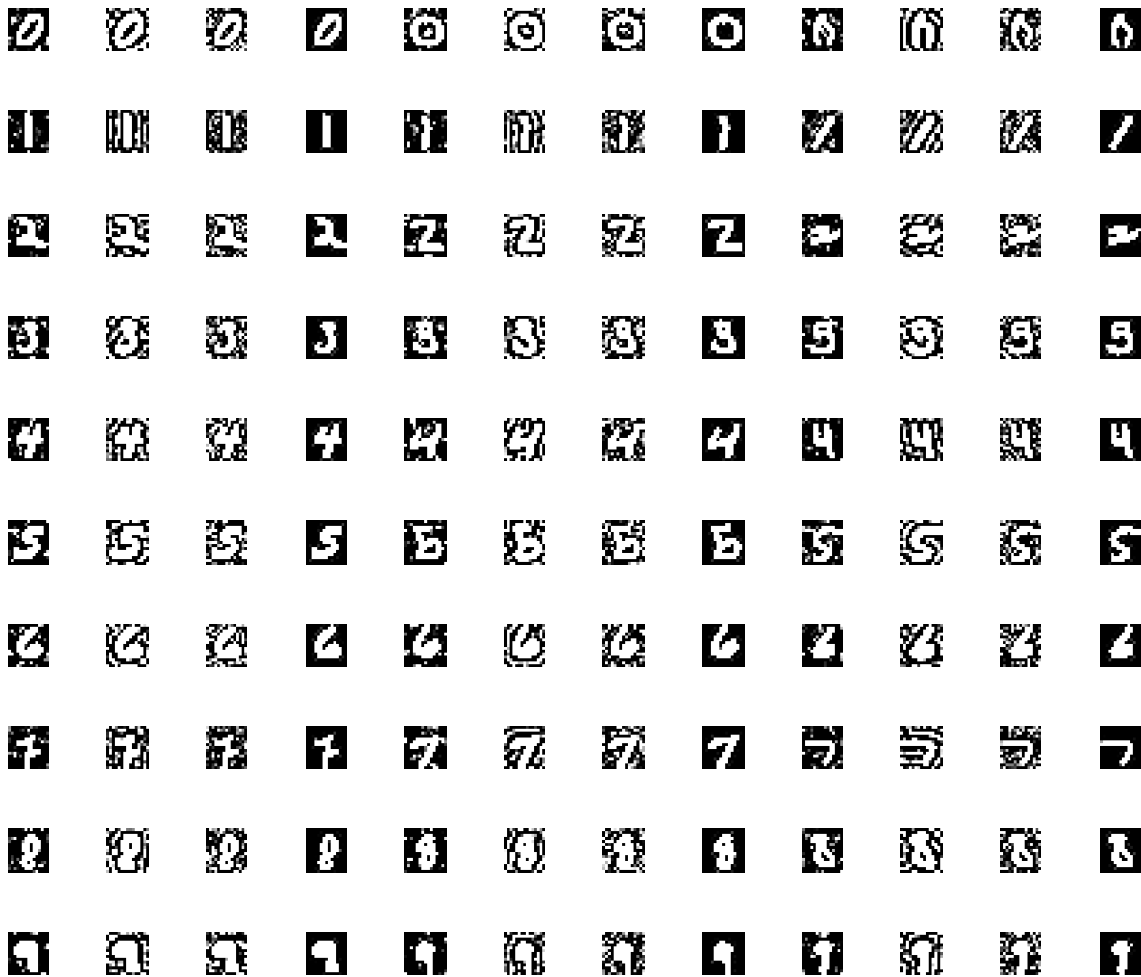


Fig. 7. We show sample images recovered from noisy ones using $B_{X_m, \alpha}$ and $B_{Y_m, \alpha'}$. Each row corresponds to a digit from 0 to 9. Every four columns consist of an example. In each example, the last image of the group is the original image and the third image is the noisy image. The first image is the one obtained by applying $B_{Y_m, \alpha'}$, while the second image is obtained by applying $B_{X_m, \alpha}$.

B. Principle components of graph signals

In this subsection, we investigate the construction of Section III by studying the principle components of graph signals. The dataset we use here is from a weather station network in the United States with $n = 197$ nodes.³ The signals are daily temperatures recorded over the year

³<http://www.ncdc.noaa.gov/data-access/>

2013.

We pre-process each f in our dataset as follows. Let c be any constant signal, we place f by $f - \langle f, c \rangle c$, i.e., the constant component from f is removed as it does not give any useful geometric information of the graph. The pre-processing step results in a perpendicular signal to the 0-smooth signals according to Definition 1.

The geographic locations of the stations are available, and based on such information, a k -NN graph $G = (V, E)$ is constructed. The size of the graph is $|V| = 194$, and the average degree of G is ≈ 5 and $|E| = 495$. Among all the signals, we randomly choose 3 samples from each month to form a sample set of signals F containing 36 signals, approximately 10% of all the available signals.

By the construction of Section III, we obtain a parametrized family of graphs $G_F : M_F \rightarrow \mathcal{G}$, where $M_F = \mathbb{R}_{\geq 0}^{37}$ and \mathcal{G} is the collection of graphs on 194 vertices. The entire image $Im(G_F)$ of G_F is too large for us to investigate. For our purpose, we consider a subset $C = \{G_0, \dots, G_{20}\}$ of $Im(G_F)$ consisting of 21 graphs. Each $G_i, 0 \leq i \leq 20$ is of the form $G_F(y_i, x_i, \dots, x_i)$ such that:

- $x_0 = 0$ (hence $G_0 = G$).
- $x_{20} \gg 1$ and $x_1 < \dots < x_{19}$ are chosen to equally divide the interval (x_0, x_{20}) .
- The control parameter y_i is chosen such that the size of G_i is approximately the same as that of G .

We first study how each $G_i, 1 \leq i \leq 20$ is different from $G_0 = G$. We compute the Hamming distance $d_H(G_0, G_i)$ that counts the number of edges contained exclusively in either G_0 or G_i . The plot of $d_H(G, G_i)$ against i is shown in Fig. 8. We see that the curve is in general increasing in i . It is steep initially and becomes flatter when i is large, say exceeds 10. For the extreme case G_{20} , it is constructed almost solely from sample signals F . However, the Hamming distance $d_H(G, G_{20})$ suggests that around 2/3 of the edges of G are also contained in G_{20} , though G and G_{20} are constructed from completely different means.

For our next task, we want to perform a Fourier analysis of the temperature signals. It is however unfavorable to use $G_i, 0 \leq i \leq 20$ directly as some of them are not connected. We construct H_i whose edges are the unions of edges in G and G_i . The plot for $d_H(G, H_i)$ is also shown in Fig. 8. For example, we add $\approx 25\%, 32\%$ more edges to G to form H_{10} and H_{20} respectively. For each $H_i, 0 \leq i \leq 20$, let L_i be its Laplacian and $B_i = \{e_{i,j}, 1 \leq j \leq 194\}$ be an eigenbasis of L_i . For each signal f , we compute its Fourier coefficients $\hat{f}_{i,j} = \langle f, e_{i,j} \rangle$. The

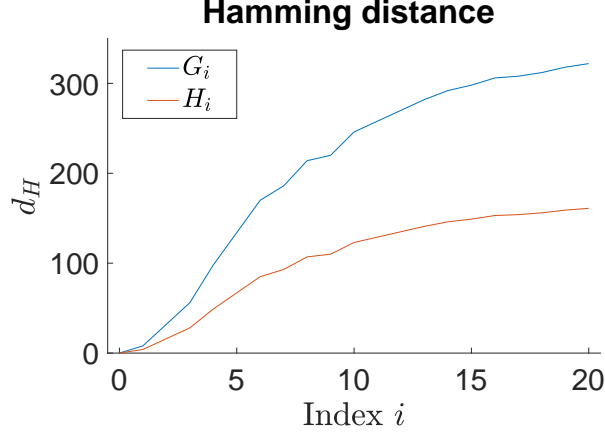


Fig. 8. The plot of Hamming distance against the index i .

principal components of f w.r.t. B_i are those indices j such that $|\hat{f}_{i,j}|$ is large. Let τ_i be the permutation of indices $\{1, \dots, 194\}$ such that $|\hat{f}_{i,\tau_i(j)}| \geq |\hat{f}_{i,\tau_i(j+1)}|$, i.e., τ_i re-orders the indices according to $|\hat{f}_{i,j}|$ decreasingly. For each $k \leq 194$, we set $\hat{f}_i^k = \sqrt{\sum_{1 \leq j \leq k} \hat{f}_{i,\tau_i(j)}^2} / |f|$. If we interpret $|f|$ as the energy of f , then \hat{f}_i^k computes the percentage of the energy of f contained in k principal components. Therefore, for the same (small) k , the H_i with larger \hat{f}_i^k value is preferred. In Fig. 9, we show the plots of average \hat{f}_i^k against k . On the left, we show the general trend by including all $1 \leq i \leq 20$ and $1 \leq k \leq 194$. We see that on the large scale, we have the same general trend for every $H_i, 0 \leq i \leq 20$. On average, for each i , \hat{f}_i^k quickly reaches a very high percentage as k increases, and the curve becomes almost flat. On the other hand, by amplifying the details for $i = 0, 10, 20$ and $k = 1, \dots, 5$, we see that H_{10} gives the largest mean \hat{f}_i^j , while H_0 gives the smallest. The graph H_{10} uses both information from the graph $G = H_0$ and the sample signals F .

While Fig. 9 gives a rough comparison, we now compare $H_0 = G$ and H_{10} in more detail. For a signal f and $1 \leq k \leq 5$, we find out $(\hat{f}_{10}^k - \hat{f}_0^k) / \hat{f}_0^k$ as the relative change against \hat{f}_0^k . We consider the change significant if either $(\hat{f}_{10}^k - \hat{f}_0^k) / \hat{f}_0^k \geq 10\%$ or $(\hat{f}_{10}^k - \hat{f}_0^k) / \hat{f}_0^k \leq -10\%$, with the former favors H_{10} and the latter favors H_0 . We go through every f in the dataset, and the distribution of instances for significant relative changes are shown in Fig. 10. We see there are much more instances that favor H_{10} than those that favor H_0 . The difference in such instances is more than 15% of the total number of signals for $k = 1$, where we use a single component to approximate a signal. It is approximately 10% for $k = 2$, where we use two components to

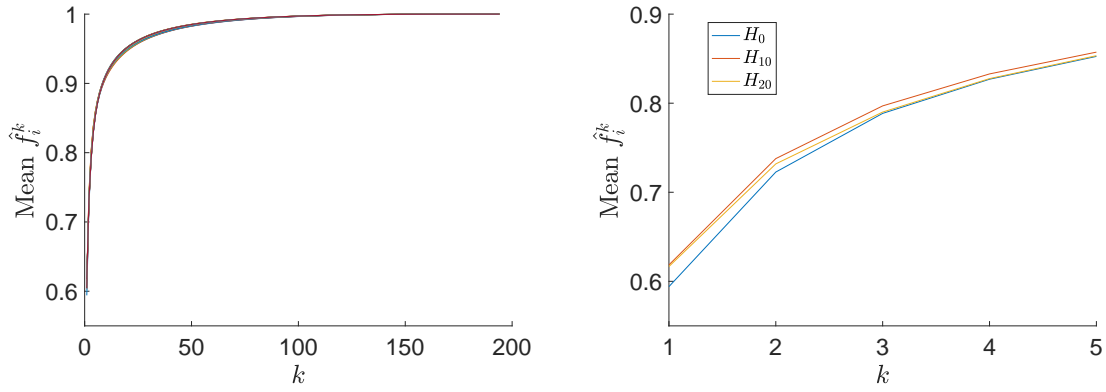


Fig. 9. The plots of mean of \hat{f}_i^k against k . On the left, we show that general trend by including all $1 \leq i \leq 20$ and $1 \leq k \leq 194$. On the right, we enlarge the details for $i = 0, 10, 20$ and $k = 1, \dots, 5$.

approximate a signal.

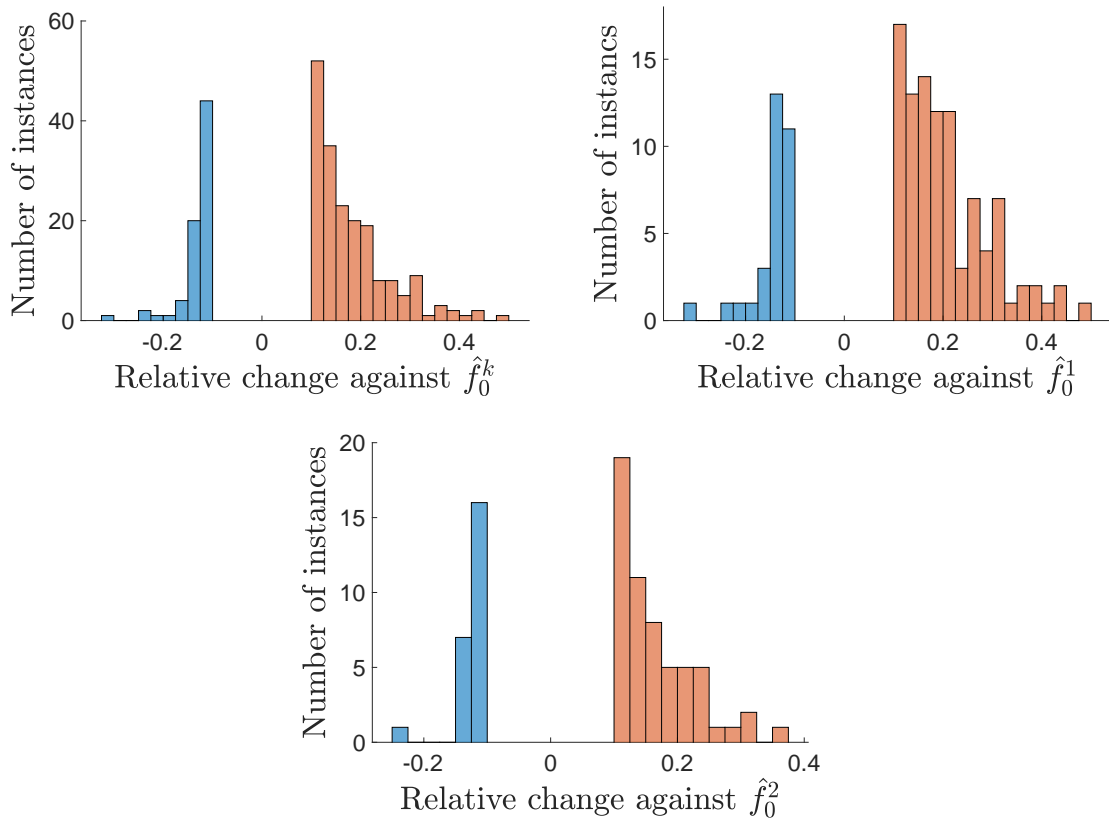


Fig. 10. The histograms of distributions of instances for significant relatives changes against \hat{f}_0^k . For the first plot, we show the results for $k = 1, 2, 3, 4, 5$ all considered together. While for the remaining two plots, we show the individual results for $k = 1$ and $k = 2$.

VI. CONCLUSIONS

In this paper, we study graph signal processing by focusing on graph signals themselves. Motivated by the necessity to understand graph signals geometrically, we introduce a new notion of smoothness. It is based on comparing a signal with a graph with both considered elements of an enlarged set of objects. The new notion allows us to partially classify graph signals, and obtain new insights in conjunction with classical GSP tools. For future works, we shall explore the potential of the framework in more application scenarios.

APPENDIX A

PROOFS OF THEORETICAL RESULTS

Proof of Lemma 1: By re-arranging indices if necessary, we assume that $f_i \leq f_{i+1}$ and $g_i \leq g_{i+1}$ for $1 \leq i \leq n - 1$. Moreover, as g is orthogonal to the constant vector, f is not orthogonal to g if and only if $f + c$ is not orthogonal to g . Without loss of generality, by adding a constant c to f if necessary, we assume that $g_i \leq f_i \leq g_{i+1}$, $1 \leq i \leq n - 1$ and $f_n \geq g_n$.

As g is nonzero and g is orthogonal to the constant vectors, we have $g_1 < 0$ and $g_n > 0$. Suppose f_i and g_i have the same parity, i.e., $f_i g_i \geq 0$, for each $1 \leq i \leq n$. As f is nonzero, either $f_1 < 0$ or $f_n > 0$. Then $\langle f, g \rangle = \sum_{1 \leq i \leq n} f_i g_i \geq \max\{f_n g_n, f_1 g_1\} > 0$.

If for some $1 \leq i \leq n$, $f_i g_i < 0$, we have $g_i < 0 < f_i$ by the interlacing property. For $j > i$, we have $f_j \geq g_j \geq f_i > 0$; while for $l < i$, we have $g_l \leq f_l \leq g_i < 0$. In particular, $f_j g_j > 0$ for each $j \neq i$. Therefore, if $1 < i < n$, we find $\langle f, g \rangle \geq f_1 g_1 + f_i g_i + f_n g_n$. As either $f_1 g_1 + f_i g_i \geq 0$ or $f_i g_i + f_n g_n \geq 0$, we have $\langle f, g \rangle > 0$. If $i = 1$ or $i = n$, then $\langle f, g \rangle \geq f_1 g_1 + f_2 g_2 + f_n g_n \geq f_2 g_2 > 0$. This concludes the proof. ■

Proof of Theorem 1: We first verify the recoverability of graphs. If G_F is as constructed, then G is nothing but $G_F(1, 0, \dots, 0)$. For recoverability of signal, we notice that

$$|f(v_i) - f(v_j)| = \inf_{x_0 \in \mathbb{R}_{\geq 0}} \{G_f(x_0, 1) \text{ contains } (v_i, v_j) \text{ as an edge}\}.$$

Therefore, if $G_f = G_{f'}$, then $|f(v_i) - f(v_j)| = |f'(v_i) - f'(v_j)|$. In the reverse direction, if $f = af' + c$, then notice that $|f(v_i) - f(v_j)| = |a||f'(v_i) - f'(v_j)|$. The equivalence between M_f and $M_{f'}$ is given by $\phi : M_f \rightarrow M_{f'}, (x_0, x_1) \mapsto (x_0, x_1/|a|)$, and $\psi : M_{f'} \rightarrow M_f, (x_0, x_1) \mapsto (x_0, |a|x_1)$.

For composability, consider two finite sets of signals F_1 of size k_1 and $F_2 = \{f_1, \dots, f_{k_2}\}$ of size k_2 . Let $F = F_1 \cup F_2$ of size k . Define $M_{1,2}$ (as an abbreviation of $(M_{F_1})_{F_2}$) to be $\mathbb{R}_{\geq 0}^{k_1+k_2+1}$.

An element of $M_{1,2}$ is denoted by $x = (x_0, y_1, \dots, y_{k_1}, z_1, \dots, z_{k_2})$ and abbreviated by (x_0, y, z) with $y = (y_1, \dots, y_{k_1})$ and $z = (z_1, \dots, z_{k_2})$. We define $G_{1,2} : M_{1,2} \rightarrow \mathcal{G}$. Given $x = (x_0, y, z)$, $G_{1,2}(x)$ is the following graph. For a pair of nodes v_i, v_j , similar to above, let

$$D_y(v_i, v_j) = \left(\inf_{x_0 \in \mathbb{R}^{\geq 0}} \{G_{F_1}(x_0, y) \text{ contains } (v_i, v_j) \text{ as an edge}\} \right).$$

From this, we compute

$$D_{y,z}(v_i, v_j)^2 = D_y(v_i, v_j)^2 + \sum_{1 \leq l \leq k_2} z_l (f_l(v_i) - f_l(v_j))^2.$$

The nodes v_i, v_j are connected by an edge in $G_{1,2}(x)$ if $D_{y,z}(v_i, v_j) \leq x_0$.

To show that $G_{1,2} \sim G_F$, recall an element of $M_{1,2}$ takes the form $(x_0, y_1, \dots, y_{k_1}, z_1, \dots, z_{k_2})$ and an element of M_F takes the form (x_0, x_1, \dots, x_k) . We examine each signal in $F_1 \cup F_2$. For $f \in F_1 \cup F_2$, assume it corresponds to y_i if $f \in F_1$, z_j if $f \in F_2$, and x_l . Then define $\phi : M_{1,2} \rightarrow M_F$ such that the x_l -component of $\phi((x_0, y_1, \dots, y_{k_1}, z_1, \dots, z_{k_2}))$ is $y_i + z_j$. It is straightforward to check that any smooth map such that $\phi \circ \psi = Id_{M_F}$ defines an equivalence between $G_{1,2}$ and G_F . ■

Proof of Proposition 1: We define the maps $\tau_1 - \tau_5$ in Fig. 4.

- For τ_1 , consider $G = (V, E) \in \mathcal{MG}_n$, define $\tau_1(G)$ to be the metric space on V with distance metric d_G on G .
- For τ_2 , given (V, d) a finite metric space on n points with metric d , define $M_V = \mathbb{R}^{\geq 0}$. For $x_0 \in M_V$, $\tau_2(V)(x_0)$ is the graph on V such that distinct pair $v_i, v_j \in V$ are connected by an edge if $d(v_i, v_j) \leq x_0$.
- For τ_3 , given $\phi : M \rightarrow \mathcal{G}_n$, the associated sequence is $Im(\phi)$ ordered by the number of edges.
- For τ_4 , let $S = \{G_1, \dots, G_k\}$ be a finite sequence of graphs on n vertices. If $k = 1$, then $\tau_4(S) = G_1$; and if $k \geq 2$, then $\tau_4(S) = G_2$.
- For τ_5 , let $f = (f_i)_{1 \leq i \leq n}$ (the notation is only valid in this proof) be an element of \mathcal{F}_n . Define $M_f = \mathbb{R}_{\geq 0}$. For $x_0 \in M_f$, $\tau_5(f)(x_0)$ is the graph on $\{v_1, \dots, v_n\}$, and v_i, v_j is connected by an edge if $|f_i - f_j| \leq x_0$.

The claims $\tau_4 \circ \tau_3 \circ \tau_2 \circ \tau_1 = Id_{\mathcal{G}_n}$ $\tau_2 \circ \tau_1(G) = G_c$ are straightforward to check for the constructions, which are omitted here. Let us verify the statement on τ_5 .

As we have seen earlier, $\tau_5(f) = \tau_5(g)$ implies that $|f_i - f_j| = |g_i - g_j|$ for any $1 \leq i \neq j \leq n$. Let us briefly recall the reason is that

$$|f_i - f_j| = \inf_{x_0 \in M_f} \{\tau(f)(x_0) \text{ contains } (v_i, v_j) \text{ as an edge}\}.$$

Subtracting f and g by the constant signals f_0 and g_0 respectively, we assume that $f_0 = g_0 = 0$. If f and g are constant signals, then we are done. Otherwise, without loss of generality, we assume that $f_2 \neq 0$ and $g_2 \neq 0$. If $f_1 = 0$ and $f_2 \neq 0$ are both fixed, then knowing $|f_i - f_1|$ and $|f_i - f_2|$ uniquely determines f_i . Therefore, as $|f_i - f_j| = |g_i - g_j|$ for any $1 \leq i \neq j \leq n$, we see that $f = g$ if $f_2 = g_2$ and $f = -g$ if $f_2 = -g_2$. ■

Proof of Lemma 2:

- 1) We notice that $*_{f+c} = *_{f}$ and $*_{rf} = r(*_{f})$ (as maps). Therefore, if f is ϵ -smooth, then so do rf and $f + c$.
- 2) Following directly from the definition, a signal of f is 0-smooth if and only if $Im(*_{f}) \subset Im(G_c)$. Suppose for 0-smooth signal f , there is an edge (v_i, v_j) such that $f(v_i) = f(v_j)$. If f is not a constant signal, then we can always find another edge (v_k, v_l) such that $f(v_k) \neq f(v_l)$ (as G is connected). Choose $0 < x < |f(v_k) - f(v_l)|$, then $*_{f}(x)$ contains (v_i, v_j) and does not contain the edge (v_k, v_l) . Hence, $*_{f}(x) \notin Im(G_c)$, and this contradicts that f is 0-smooth.

Suppose G is a path graph on $n \geq 2$ vertices. We order the vertices as v_1, \dots, v_n from one end to the other. Then the non-constant signal $f = (1, \dots, n)^T$ is also 0-smooth.

Conversely, suppose G is not a path graph and f is a non-constant 0-smooth signal. According to the first paragraph, for each edge (v_i, v_j) of G , $f(v_i) \neq f(v_j)$. We consider two cases, G is a tree and G contains a cycle.

Case 1: If G is a tree, then it must contain a node of degree at least 3, say v_1 . Without loss of generality, assume that 3 of its neighbors are v_2, v_3 , and v_4 . If $|f(v_i) - f(v_1)|, i = 2, 3, 4$ are not the same, then re-ordering if necessary we may assume $|f(v_2) - f(v_1)| < x < |f(v_3) - f(v_1)|$ for some x . Then $*_{f}(x)$ contains (v_1, v_2) as an edge and excludes (v_1, v_3) . Hence, $*_{f}(x) \notin Im(G_c)$ and this is a contradiction. If $|f(v_i) - f(v_1)|, i = 2, 3, 4$ are all equal to y , then for at least two nodes, say v_2, v_3 , we have $f(v_2) = f(v_3)$. Choose $0 < x < y$, we have $*_{f}(x)$ contains (v_2, v_3) as an edge but excludes both (v_1, v_2) and (v_2, v_3) . Hence, $*_{f}(x) \notin Im(G_c)$ and this leads to a contradiction.

Case 2: If G contains a cycle of size $m \geq 3$. We order the vertices along the cycle as v_1, \dots, v_m . If there are pairs (v_i, v_{i+1}) and (v_j, v_{j+1}) with $i \neq j$ (by convention, $v_{m+1} = v_1$), such that $|f(v_i) - f(v_{i+1})| < x < |f(v_j) - f(v_{j+1})|$, then $*_f(x)$ contains (v_i, v_{i+1}) as an edge and excludes (v_j, v_{j+1}) . This is impossible if we want $*_f(x) \notin \text{Im}(G_c)$. Therefore, $|f(v_i) - f(v_{i+1})|$ equals to some $y \neq 0$ for every $1 \leq i \leq m$. This can only happen that for some $i \neq j$, $f(v_i) = f(v_j)$. Consider $0 < x < y$, $*_f(x)$ contains (v_i, v_j) as an edge but excludes (v_1, v_2) . Hence $*_f(x) \notin \text{Im}(G_c)$ and the contradiction concludes the last subcase.

3) Notice that in the expression (1) of d_S with $\gamma_1 = *_f$ and $\gamma_2 = G_c$, the d_H factor in each term is uniformly bounded by $2n^2$ independent of f . Moreover, fix a non-constant signal f , for any signal f' such that $\|f - f'\| \leq \epsilon$ for ϵ small enough, we can always ensure that

- (a) f' is non-constant.
- (b) The part $1/|\gamma_1'^{-1}(\text{Im}(\gamma_1')^\circ)|$ has an upper bound α that depends only on f for any ϵ small enough.
- (c) For any $G \in \text{Im}(\gamma_1)^\circ \cup \text{Im}(\gamma_1')^\circ$, $||\gamma_1^{-1}(G)| - |\gamma_1'^{-1}(G)||$ is bounded by $\beta(\epsilon)$ that converges to 0 if $\epsilon \rightarrow 0$.

We also notice that the number of graphs in $\text{Im}(\gamma_1)^\circ \cup \text{Im}(\gamma_1')^\circ$ is also bounded by n^2 , which is independent of both f and ϵ . Now we estimate

$$|d_S(\gamma_1, \gamma_2) - d_S(\gamma_1', \gamma_2)| \leq n^2 \cdot \beta(\epsilon) \cdot 2\alpha \cdot 2n^2 = 4n^4 \alpha \beta(\epsilon) \rightarrow 0,$$

as $\epsilon \rightarrow 0$. ■

Proof of Proposition 2: Let $\gamma_1 = *_f$, $\gamma_2 = G_c$ and ordered sequence of pairs of vertices $Q = (Q_l)_{1 \leq l \leq n(n-1)/2}$ as earlier. As we assume that $|f(u_1) - f(v_1)| \neq |f(u_2) - f(v_2)|$, the image $\text{Im}(\gamma_1)$ of γ_1 is a sequence of graphs $G_{(l)}$, $1 \leq l \leq n(n-1)/2$ such that the edge set of $G_{(l)}$ is $\{Q_l, 1 \leq l \leq l\}$, i.e., $G_{(l+1)}$ is obtained from $G_{(l)}$ by adding Q_{l+1} . To compute ϵ , we need to find $d_H(G_{(i)}, G^{(j)})$ for suitable $1 \leq i \leq n(n-1)/2$ and $0 \leq j \leq k$. In doing so, we may take the sum over all the edges of $G_{(i)}$ and $G^{(j)}$, i.e., $d_H(G_{(i)}, G^{(j)}) = \sum_{1 \leq l \leq n(n-1)/2} \theta_{i,j}(Q_l)$, where $\theta_{i,j}(Q_l) = 1$ if Q_l is an edge of either $G_{(i)}$ or $G^{(j)}$ exclusively and 0 otherwise. Therefore, ϵ is expressed in the form $\sum_{G_{(i)}, G^{(j)}} \sum_{Q_l} \theta_{i,j}(Q_l)$. We want to change the summation order $\sum_{Q_l} \sum_{G_{(i)}, G^{(j)}} \theta_{i,j}(Q_l)$. This prompts us to go through Q_l one-by-one and study its membership in $G_{(i)}$ and $G^{(j)}$. With this perspective, we describe an equivalent formula for $\epsilon_{\mathcal{P}}$.

For the partition \mathcal{P} of I , we claim that

$$\epsilon_{\mathcal{P}} = \sum_{0 \leq j \leq D_G} \sum_{i \in I_j} \frac{\gamma_1^{-1}(G_{(i)})}{\gamma_1^{-1}(Im(\gamma_1)^\circ)} d_H(G_{(i)}, G^{(j)}). \quad (2)$$

We prove the claim by showing that for each pair of nodes $Q_l = \{u_l, v_l\}$, $1 \leq l \leq n(n-1)/2$, it contributes to the same summand on both sides of (2). For the left-hand-side, the contribution of Q_l is ϵ_l . On the right-hand-side, Q_l contributes to either 1 or 0 in each of $d_H(G_{(i)}, G^{(j)})$. We notice that $G_{(i)}$ is a subgraph of $G_{(i+1)}$ and similarly $G^{(j)}$ is a subgraph of $G^{(j+1)}$. The pair Q_l is an edge of $G_{(i)}$ for $i \geq l$. Let k be the smallest index such that Q_l is an edge of $G^{(k)}$. Then Q_l is an edge of $G^{(j)}$ for $j \geq k$. Therefore, Q_l contributes 1 to $d_H(G_{(i)}, G^{(j)})$ with $i \in I_j$ if and only if:

- (a) $i < l$ and $j \geq k$, or
- (b) $i \geq l$ and $j < k$.

Let l' be smallest index such that $Q_{l'} \in G^{(k)}$ and $l \in I_{k'}$. Correspondingly, we consider two cases on k and k' (illustrated in Fig. 11):

- (a') If $k \leq k'$, then (b) cannot happen. For if $i \geq l$, then $i \notin I_j$ as $j < k \leq k'$. Therefore $i < l$ and $j \geq k$. The condition $i \in I_j$ together with $j \geq k$ imply that $i \geq l'$. In summary, we have $l' \leq i < l$ and $k \leq j \leq k'$ such that $i \in I_j$. Therefore, the contribution of Q_l to the right-hand-side of (2) is $\frac{\sum_{l' \leq i < l} \gamma_1^{-1}(G_{(i)})}{\gamma_1^{-1}(Im(\gamma_1)^\circ)}$, which is exactly ϵ_l as $\gamma_1^{-1}(G_{(i)}) = |f(u_{i+1}) - f(v_{i+1})| - |f(u_i) - f(v_i)|$.
- (b') If $k > k'$, then (a) cannot happen. We can show that the contribution of Q_l to the right-hand-side of (2) is ϵ_l by the exact same argument.

This completes the proof of (2).

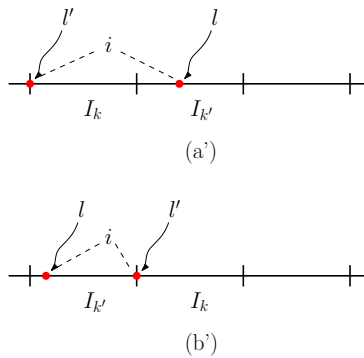


Fig. 11. An illustration of the proof of (2).

If we examine the definition of ϵ , for each $0 \leq j \leq D_G$, define I'_j as follows: an index $1 \leq l \leq n(n-1)/2$ belongs to I'_j if $d_H(G_{(l)}, G^{(j')}) > d_H(G_{(l)}, G^{(j)}) = d_H(G_{(l)}, \text{Im}(\gamma_2))$ for any $j' > j$. We claim that $\mathcal{P}' = \{I'_j, 0 \leq j \leq D_G\}$ is a partition of Q .

For any $1 \leq l \leq n(n-1)/2$, suppose l is associated with j and $l+1$ is associated with j' as described in the previous paragraph. To prove the claim, it suffices to show that $j \leq j'$. Suppose on the contrary that $j' < j$. From the definition, we have $d_H(G_{(l)}, G^{(j)}) \leq d_H(G_{(l)}, G^{(j')})$ and $d_H(G_{(l+1)}, G^{(j')}) < d_H(G_{(l+1)}, G^{(j)})$. Notice that $G_{(l+1)}$ is obtained from G_l by including a single edge Q_{l+1} . We consider the following cases:

- (i) $Q_{l+1} \in G^{(j')}$: In this case, Q_{l+1} is also in $G^{(j)}$. Hence, $d_H(G_{(l)}, G^{(j)}) - 1 = d_H(G_{(l+1)}, G^{(j)})$ and $d_H(G_{(l)}, G^{(j')}) - 1 = d_H(G_{(l+1)}, G^{(j')})$. This gives a contradiction, as

$$d_H(G_{(l+1)}, G^{(j)}) = d_H(G_{(l)}, G^{(j)}) - 1 \leq d_H(G_{(l)}, G^{(j')}) - 1 = d_H(G_{(l+1)}, G^{(j')}).$$

- (ii) $Q_{l+1} \notin G^{(j)}$: We also have $Q_{l+1} \notin G^{(j')}$. Hence, $d_H(G_{(l)}, G^{(j)}) + 1 = d_H(G_{(l+1)}, G^{(j)})$ and $d_H(G_{(l)}, G^{(j')}) + 1 = d_H(G_{(l+1)}, G^{(j')})$. We have the same contradiction as in (i).

- (iii) $Q_{l+1} \in G^{(j)}$ and $Q_{l+1} \notin G^{(j')}$: In this case, we have $d_H(G_{(l)}, G^{(j)}) - 1 = d_H(G_{(l+1)}, G^{(j)})$ and $d_H(G_{(l)}, G^{(j')}) + 1 = d_H(G_{(l+1)}, G^{(j')})$. The equations imply that $d_H(G_{(l+1)}, G^{(j)}) < d_H(G_{(l+1)}, G^{(j')})$, which is again a contradiction.

The three cases conclude our proof of the claim by contradiction.

In defining the partition \mathcal{P}' , for the pair l and I'_j , we have $d_H(G_{(l)}, G^{(j)}) = d_H(G_{(l)}, \text{Im}(\gamma_2))$. Therefore for \mathcal{P}' , we have $\epsilon = \epsilon_{\mathcal{P}'}$, in view of (2). For any other partition $\mathcal{P} = \cup_{0 \leq k \leq D_G} I_k$, if $i \in I_{j'}$, then $d_H(G_{(l)}, G^{(j')}) \geq d_H(G_{(l)}, \text{Im}(\gamma_2)) = d_H(G_{(l)}, G^{(j)})$. Therefore, $\epsilon_{\mathcal{P}} \geq \epsilon_{\mathcal{P}'}$. ■

REFERENCES

- [1] D. I. Shuman, B. Ricaud, and P. Vandergheynst, "A windowed graph fourier transform," in *Proc. IEEE Workshop on Statistical Signal Process.*, 2012.
- [2] D. I. Shuman, S. K. Narang, P. Frossard, A. Ortega, and P. Vandergheynst, "The emerging field of signal processing on graphs: Extending high-dimensional data analysis to networks and other irregular domains," *IEEE Signal Process. Mag.*, vol. 30, no. 3, pp. 83–98, 2013.
- [3] A. Sandryhaila and J. M. F. Moura, "Discrete signal processing on graphs," *IEEE Trans. Signal Process.*, vol. 61, no. 7, pp. 1644–1656, 2013.
- [4] —, "Big data analysis with signal processing on graphs: Representation and processing of massive data sets with irregular structure," *IEEE Signal Process. Mag.*, vol. 31, no. 5, pp. 80–90, 2014.
- [5] A. Gadde, A. Anis, and A. Ortega, "Active semi-supervised learning using sampling theory for graph signals," in *Proc. ACM SIGKDD Int. Conf. on Knowledge Discovery and Data Mining*, 2014.

- [6] X. Dong, D. Thanou, P. Frossard, and P. Vandergheynst, "Learning Laplacian matrix in smooth graph signal representations," *IEEE Trans. Signal Process.*, vol. 64, no. 23, pp. 6160–6173, 2016.
- [7] M. Defferrard, X. Bresson, and P. Vandergheynst, "Convolutional neural networks on graphs with fast localized spectral filtering," in *NeurIPS*, 2016.
- [8] T. N. Kipf and M. Welling, "Semi-supervised classification with graph convolutional networks," in *ICLR*, 2017.
- [9] H. E. Egilmez, E. Pavez, and A. Ortega, "Graph learning from data under Laplacian and structural constraints," *IEEE J. Sel. Top. Signal Process.*, vol. 11, no. 6, pp. 825–841, 2017.
- [10] F. Grassi, A. Loukas, N. Perraudin, and B. Ricaud, "A time-vertex signal processing framework: Scalable processing and meaningful representations for time-series on graphs," *IEEE Trans. Signal Process.*, vol. 66, no. 3, pp. 817–829, 2018.
- [11] A. Ortega, P. Frossard, J. Kovačević, J. M. F. Moura, and P. Vandergheynst, "Graph signal processing: Overview, challenges, and applications," *Proc. IEEE*, vol. 106, no. 5, pp. 808–828, 2018.
- [12] B. Girault, A. Ortega, and S. S. Narayanan, "Irregularity-aware graph fourier transforms," *IEEE Trans. Signal Process.*, vol. 66, no. 21, pp. 5746–5761, 2018.
- [13] F. Ji and W. P. Tay, "A Hilbert space theory of generalized graph signal processing," *IEEE Trans. Signal Process.*, vol. 67, no. 24, pp. 6188 – 6203, 2019.
- [14] A. Agaskar and Y. M. Lu, "A spectral graph uncertainty principle," *IEEE Trans. Inf. Theory*, vol. 59, no. 7, pp. 4338–4356, 2013.
- [15] S. Chen, R. Varma, A. Sandryhaila, and J. Kovačević, "Discrete signal processing on graphs: Sampling theory," *IEEE Trans. Signal Process.*, vol. 63, no. 24, pp. 6510–6523, 2015.
- [16] M. Tsitsvero, S. Barbarossa, and P. Di Lorenzo, "Signals on graphs: Uncertainty principle and sampling," *IEEE Trans. Signal Process.*, vol. 64, no. 18, pp. 4845–4860, 2016.
- [17] A. G. Marques, S. Segarra, G. Leus, and A. Ribeiro, "Sampling of graph signals with successive local aggregations," *IEEE Trans. Signal Process.*, vol. 64, no. 7, pp. 1832–1843, 2016.
- [18] A. Anis, A. Gadde, and A. Ortega, "Efficient sampling set selection for bandlimited graph signals using graph spectral proxies," *IEEE Trans. Signal Process.*, vol. 64, no. 14, pp. 3775–3789, 2016.
- [19] D. E. O. Tzamaras, P. Akyazi, and P. Frossard, "A novel method for sampling bandlimited graph signals," in *Proc. 26th European Signal Process. Conf.*, 2018.
- [20] R. Varma and J. Kovačević, "Random sampling for bandlimited signals on product graphs," in *Proc. 13th Int. Conf. Sampling Theory and Applications*, 2019.
- [21] B. Le Bars, P. Humbert, L. Oudre, and A. Kalogeratos, "Learning laplacian matrix from bandlimited graph signals," in *Proc. IEEE Int. Conf. Acoustics, Speech and Signal Process.*, 2019.
- [22] F. Ji, H. Feng, H. Sheng, and W. P. Tay, "Sampling theory of bandlimited continuous-time graph signals," *arXiv preprint arXiv:2010.09952*, 2020.
- [23] G. Carlsson, "Topology and data," *Bull. Amer. Math. Soc.*, no. 46, pp. 255–308, 2009.